Modelling of Pickup Ion Distributions in the Halley Cometosheath: Empirical Rates of ionization, Diffusion, Loss and Creation of Fast Neutral Atoms

D. E. HUDDLESTON, M. NEUGEBAUER, AND B. E. GOLDSTEIN

Jet Propulsion Laboratory, California Institute of Technology, Pasadena, California

for submission to *Journal of Geophysical Research*
December 1993

Abstract

The shape of the velocity distribution of water-group ions observed by the Giotto ion mass spectrometer on its approach to comet Hal Icy is modeled to derive empirical values for the rates of ionization, energy diffusion, and loss in the mid-cometosheath. The model includes the effect of rapid pitch-angle scattering into a bispherical shell distribution as wc]] as the effect of the magnetization of the plasma on the charge-exchange loss rate. It is found that the average rate of ionization of cometary neutrals in this region of the cometosheath appears to be roughly a factor of 3 faster than the standard rates of -1 x10-6 s-1 that arc usual] y used in theoretical comet models to give results consistent with observations in most regions of the comet environment. For the region of the coma studied (1.2-1.8x105 km from the nucleus), the energy diffusion coefficient was D_o = 0.005 km^2s^{-3}, which is lower than values used in models of other regions of the coma. The empirically obtained loss rate appears to be an order of magnitude or more greater than can be explained by charge exchange with the standard cross-sections of -2x1 0^{-15} cm^2. If the entire loss rate is due to charge exchange then the implied rate of creation of fast neutral atoms is of the order ~10^{-4} s]. The fast atoms may, in turn, be partly responsible for the higher-than-expected ionization rate.

1. INTRODUCTION

When a comet approaches the *Sun,* the volatile cometary material is heated and sublimes from the surface of the nucleus. The gas is predominantly of the water group (~80% [*Krankowsky et al., 1986]*) which sublimes essentially at the surface, although of the minor constituents, CO and formaldehyde possibly originate from an extended source [*Eberhardt et al., 1987; Meier et al., 1993]. The* neutral gas undergoes chemical and photochemical processes in the collision-dominated inner coma, and expands with its thermal velocity, V_e - *1* km/s, to distances of up to ~10^6 -107 km from the nucleus. It is ionized both by solar photons and as a result of charge exchange with solar-wind and picked-up cometary ions.

In the upstream regions the newly-born cometary ions arc initially injected into the flowing plasma at the local solar wind speed, $|\mathbf{v}_{inj}| = u_{sw}$ in the solar wind frame, where $V_e << u_{sw}$ *is* neglected, Their direction is antiparallel to $\mathbf{u}_{sw}$, so (hat their initial pitch angle is given by $\cos\theta$ =- -cm *a* where α is the angle between $\mathbf{u}_{sw}$ anti the interplanetary magnetic field, **B**. The component of $\mathbf{v}_{inj}$ perpendicular to **B** is rapidly converted to a gyration about the field lines duc to the Lorentz force, and the implanted ions initially form a ring-beam in velocity space, travelling upstream along **B** with speed $v_{\|} = -u_{sw} \cos\alpha$ *in* the solar wind frame. This distribution is unstable to the generation of Alfvénic turbulence [*Wu and Davidson, 1972; Galeev,* 1986; *Sagdeev et* al., 1986] with which the pickup ions interact to become scattered from a ring-beam toward a shell-]ike (distribution in velocity space. The likely asymptotic pitch angle distribution is the bispherical shell [*Galeev and Sagdeev*, 1988; *Huddleston and Johnstone, 1992],* comprising the low-energy portions of characteristic surfaces centered on the parallel - propagating Alfvén wave velocities $\pm V_A$ and intersecting at $\mathbf{v}_{inj}$. Development of a bispherical shell distribution is supported by observations of pickup ions near the bow shock [*Coates et al.*, 1 990] and in the midcometosheath [*Huddleston et al.,* 1993] at

comet Halley, by good agreement of the predicted wave spectrum with that observed [*Huddleston and Johnstone, 1992.],* and by numerical calculations of ion pitch angle scattering [*Miller et* a/., 1991; *Huddleston et* al., 1 *992].*

Close to the nucleus, in the cometosheath regions where the implanted heavy cometary ions begin to dominate the mass flux, the center-of-mass plasma frame shifts to approximately the bulk speed, $\mathbf{u}_{wg}$, of the water group ions and the magnetic field is then "frozen in" with $\mathbf{u}_{wg}$ rather than with $\mathbf{u}_{sw}$. Thus particles which become newly ionized within this region are picked up in the $\mathbf{u}_{wg}$ frame with initial speed $|\mathbf{u}_{wg}|$. As the plasma flow slows and magnetic field pileup begins, the Alfvén speed becomes an appreciable fraction of the flow speed and the geometry of the bispherical shell in this case is significantly different from a spherical shell, as i 1 lust rated in Figure 1 (from *Huddleston et al.* [1993]).

In the midcometosheath region near the magnetic pileup boundary of comet Halley, the observed cometary ion densities increase to unexpectedly high levels [*Neugebauer et al.,* 1991; *Altwegg et al., 1993]* and cannot at present be accounted for by even the most sophisticated models [e.g., *Schmidt et al., 1988].* Among the suggested explanations are the possibility of a temporarily increasing gas emission rate, emission from dust grains, increased electron impact ionization rate caused by adiabatical 1 y heated trapped electrons (postulated for the "mystery region" by *Larson and Lin* [1992]), and electron knock-out collisions by high-momentum heavy neutrals.

in the present paper wc examine and model the water-group ion velocity distributions observed by the high energy range spectrometer (HERS) of the Giotto ion mass spectrometer (IMS), and investigate the losses of ions at energies above the injection peak. One possible explanation is that a few of the accelerated pickup ions undergo recombination or charge exchange with the cometary neutral population and arc thereby a source of fast neutral particles which may participate in further interactions in the inner cometary regions. Unlike the charged solar wind and pickup particles, the fast

neutrals may enter the magnetic field-free cavity and their subsequent reionization may contribute to the unexpected flux of fast heavy ions observed in the cavity [*Eviatar et al., 1989*]. Possible effects of fast neutrals also include creation of the observed flux of negative ions, and the creation of additional positive ions which may help explain the discrepancy between observed and expected ion density.

2. THE IONIZATION RATE

The first step before modelling the IMS ion distributions is to derive an expression for the ionization of cometary gas for use in the transport equation. A simple, spherically symmetric outgassing model is taken for the density of cometary neutrals at a distance r from the nucleus:

$$N_c = \frac{Q}{4\pi V_e r^2} \exp\left(-\frac{\nu_i r}{V_e}\right) \tag{1}$$

where Q is the gas production rate, ν_i is the ionization rate, and V_e is the gas expansion velocity ≈ 1 km/s for the heavy particles. The implanted cometary ion density n_i can be estimated by integrating the ion production rate upstream (Sunward) along the ion flowline from the local observation position (x_0, y_0, z_0), to give

$$n_i = \frac{1}{u_{wg}} \int N_c \nu_i \, ds = \frac{1}{u_{wg}} \int_{x_0}^{\infty} \frac{Q \nu_i}{4\pi V_e r^2} \exp\left[-\frac{\nu_i r}{V_e}\right] ds \tag{2}$$

where u_{wg} is the implanted ion bulk flow speed in the cometosheath region of interest.

Figure 2 shows the IMS HERS water group ion densities, together with the profile calculated from equation (2) for $Q_{H_2O} = 5.5 \times 10^{29}$ /s as found from the Giotto neutral mass spectrometer [*Krankowsky et al., 1986*] and vi -3 x 10^{-6} /s for the best fit.

Although the detailed shape of the profile is not as observed, the modelled ion density is of the right order. The ν_i obtained is greater than the values -1 X 10^{-6}/s generally used (for photoionization plus charge-exchange) in standard models and suggests an enhanced ionization rate in this region of the 1 Halley environment. While it is conceivable that a temporal increase in Q could in error be compensated for in the model by a higher ν_i in order to fit the density observations (see also the discussion in *Hodges*[1990]), the same Q_{H_2O} = 5.5x 102' /s [*Krankowsky et al., 1986]* fits the neutral density profile (as will be discussed in the summary section). Since Q and ν_i occur differently in the expressions for N_c and n_i, then changing Q and ν_i in the model would not be likely to give a good fit to both profiles simultaneously. Another possible uncertainty is that for an expanding gas with a distribution of velocities (averaging at ~1km/s) the slower neutrals take longer to reach a given distance and so if they arc depleted first, a higher (ν_i/V_e) would be misinterpreted as higher vi by a constant V_e model. For the low H_2O temperatures, however, such an effect is expected to be small,

The effect of fast neutrals on the ionization rates is an interesting consideration since there is indirect evidence for fast neutrals in observation of fast reionized neutral great-granddaughters within the magnetic cavity, and there is also apparently a significant energetic ion loss occurring from the observed ion distributions. Four example plots in Figure 3 each show sequential pairs of distributions along the inbound Giotto trajectory. The distributions arc in 6.25 km/s v-shell bins. The distribution at the greater distance from the nucleus (dashed line) of each pair has a higher phase space density than the closer distribution for some of the v-bins above $|v_{inj}|$. This is contrary to what is expected particularly if injected source ions arc accelerated by energy diffusion (and perhaps adiabatic compression). The shaded areas represent a first approximation to the density lost between successive distributions, A better estimate can be attempted by modelling the acceleration processes affecting the ions, which, in the absence of any loss would be expected to increase the density of ions at $v > |v_{inj}|$ as the distribution convects

toward the Comet. The aim of the present paper is to examine the ion source and loss rates, and provide empirical estimates of the fast neutral production, as a step toward understanding the observations in the midcometosheath region. (A full chemical model and explanation of the enhanced ion densities is beyond the scope of the present work.)

3. MODELLING OF ION VELOCITY DISTRIBUTIONS

The sketch in Figure 4 illustrates the effects we wish to model in the evolution of the cometary ion spectra: (*a*) The continual pickup of new cometary ions at $\mathbf{u}_{wg}$ (where $\mathbf{u}_{wg}$ is decelerating along the flowline) and rapid pitch-angle scattering to form a bispherical injection shell with peak $F(v)$ at average radius significantly less than $v = |\mathbf{u}_{wg}|$ in the plasma frame [*Huddleston et al., 1993]*. (b) Energy diffusion broadens the peak. (*c*) Charge exchange (or other depiction process) removes fast ions.

The water group ion distributions at distances ~1 to 2 Xl 0^5 km from the nucleus are taken in pairs (see examples in Figure 3). Distribution 1 (the greater r, lower n_i distribution of a given pair) is taken as the starting point for the numerical run, from which distribution 2 is to be modelled. First of all, each of the 6.25 km/s bins are divided up into smaller bins and the F(v) interpolated between them, in order to provide a better numerical resolution for the purposes of running the model. Then, since the observations are along the Giotto path (approaching at ~10°7.2° to the Sun-comet line), it is necessary to "project" the. position of distribution 1 to a position 1' directly upstream from distribution 2 at which the implanted ion density (according to the model) is equivalent. Figure 5 illustrates the geometry involved. This enables the transport of implanted ions along the flowline (alongs) to be considered.

The transport equation used for the velocity-space distribution $F(v)$ is:

$$u_{wg}\frac{\partial F}{\partial s} = -\frac{N_c\,\nu_i\,g(v)}{\sum_{v\ bins} 4\pi v^2\ g(v)\ dv} + \frac{1}{v^2}\frac{\partial}{\partial v}\left[v^2 D_{vv}\frac{\partial F}{\partial v}\right] - v'\,\sigma\,N_c\,F \qquad (3)$$

Each term describes a rate of change to F and has units phase space density per second. The term on the left hand side approximates the steady-state convection of ions along the flowline. For u_{wg} a linear fit (u_{wg} :-0.0002 r) to the IMS velocity measurements (data presented by *Altwegg et al.* [1993]) is used for r equal to distance in km along the Giotto trajectory. On the right hand side, the source term puts the ion production rate into a Gaussian distribution of the form [e.g., *Puhl et al.*, 1993]

$$g(v) = C\exp\left[-\frac{(v - \langle|v|\rangle_{inj})^2}{\delta^2}\right] \qquad (4)$$

with Gaussian width δ. Since a velocity distribution is required for the source to $F(v)$ and a bispherical shell has a significant v-width [*Huddleston et al.*, 1993] the effect of the rapid pitch-angle scattering to the injection v-distribution needs to be included in the source term. The velocity distribution of the ideal thin bispherical shell varies between a maximum radius of $|u_{wg}|$ at the point of injection down to the minimum radius $VU - V_A$ on the $+v_{||}$ axis (see Figure 1) where $V_u^2 = u_{wg}^2 \sin^2 \alpha + (u_{wg}\cos\alpha - V_A)^2$ is the radius of the $-V_A$-centered partial shell. The Gaussian full width is therefore required to be approximately the v-width, A, of the bispherical distribution, $\delta = A/2 = \frac{1}{2}(u_{wg} - VU + V_A)$, which may be calculated using average values of α and V_A in the region of interest (see *Huddleston et al.* [1993]). The average velocity radius of the bispherical shell is $\langle|v|\rangle_{inj}$ in the u_{wg} frame, which is significantly less than $|u_{wg}|$ and found to be in reasonable agreement with the observed peak injection velocity [*Huddleston et al., 1993*]. For the present model, the distribution peak values presented in Figure 6 of *Huddleston et al.*

[1 993] are interpolated to provide the injection shell υ for positions between distributions in the model run.

The second term on the right-hand side of equation (3) describes the rate of change of F under quasilinear velocity-space diffusion due to resonant wave-particle interactions. For the diffusion coefficient, $D_{\upsilon\upsilon}$, a v-dependence is included which reflects the frequency (and hence velocity) dependence of the pov er spectrum of resonant waves (see *Isenberg [1987]* and equation (1 O) of *Gombosi et al.* [988])

$$D_{\upsilon\upsilon} = D_0 \left(\frac{\upsilon}{\upsilon_0} \right)^{\gamma - 1} \tag{5}$$

where γ is the wave spectra' index, and y = *2* is appropriate at Halley [*Glassmeier et al.*, 1989; *Huddleston and Johnstone, 1992].* υ_0 = 20 km/s is used, and D_0 is a constant adjusted in the mode] to give an empirical level of diffusion.

Quasi-] inear theory is not strictly valid for high levels of turbulence as found near and within the bow shock. Nevertheless, velocity diffusion is important in the cometosheath region of interest (pitch-angle scattered distributions are observed) and therefore it is included in the model. An adiabatic term is not included. It is not clear how important it is in this region of the cometosheath, and this will depend on how the flow is decelerated and deflected around the contact surface. In regions further upstream, the adiabatic effect is probably small in comparison to the effect of wave-particle diffusion except in the vicinity of large jumps in flow speed, such as at the bow shock. In modelling of distributions outside the bow shock [*Huddleston* et al., 1992.; *Ye et al.*, 1993] it was found that adiabatic effects can safely be ignored. However, it should be kept in mind that its inclusion would require an increase of the ion depletion rates necessary to fit the observations. Also it is assumed that the difference between neighbouring flow] ines is small in comparison to the changes along them, which is an

approximation sine.c the implanted ion density along the flowline increase s faster for flowlines closer to the Sun-cored line. Therefore there may be some effect (which we have ignored) on diffusion levels because the more quickly accumulated ion distributions would have less time to interact with the wave field.

The loss term in equation (3) is written in terms of charge exchange of ions with the outgassing neutrals, where σ is the cross-section for the process. This is not the only possible ion depletion mechanism, for example, some may be lost through recombination, some may also be annihilated by collisions with dust, and some may charge-exchange with fast particles neutralized previously (which may have become decelerated due to ncu[ra]-neutral collisions). Fitting σ and comparing with the generally used cross-section of $\sigma \sim 2 \times 10^{-15}\,\mathrm{cm}^2$ [e.g., *Mukai et al.*, 1986; *Huddleston at al.*, 1990; *Puhl et al.*, *1993* and references therein] gives an idea of the magnitude of the effect.

In calculation of the charge exchange rates the average velocity magnitude, $v' = \langle |\mathbf{u}_{wg} + \mathbf{v}| \rangle$, of the ions with respect to the neutrals (neglecting V_e) *is* calculated over the whole shell (assuming a spherical shell for this approximation) to include the ion gyration velocity. Thus the increased ion pathlength caused by the magnetization of the plasma is taken into account by means of the average velocity magnitude v'. A constant phase space density around the shell is assumed (i.e., wc assume gyrotropy and isotropy). For a given velocity shell radius (corresponding to one particular v-bin in $F(v)$), the vector magnitude

$$|\mathbf{u}_{wg} + \mathbf{v}| = \left[(v \sin\theta)^2 + (u_{wg} - v\cos\theta)^2\right]^{1/2} = \left[v^2 + u_{wg}^2 + 2u_{wg} v \cos\theta\right]^{1/2} \qquad (6)$$

must be averaged over the spherical surface of radius $|\mathbf{v}|$ centered on $|\mathbf{u}_{wg}|$. This is done by considering an elemental annulus of radius v sin θ, width v $d\theta$ on the shell surface, and integrating over all annuli for θ = O to π around the shell. The integration is

$$v' = \langle |\mathbf{u}_{wg} + \mathbf{v}| \rangle = \frac{\int_{\pi}^{0} 2\pi v^2 F(v) \left[v^2 + u_{wg}^2 + 2u_{wg} v \cos\theta \right]^{1/2} \sin\theta \, d\theta}{\int_{\pi}^{0} 2\pi v^2 F(v) \sin\theta \, d\theta} \qquad (7)$$

which gives

$$v' = \frac{1}{6u_{wg}v} \left[(v^2 + u_{wg}^2 + 2u_{wg} v)^{3/2} - (v^2 + u_{wg}^2 - 2u_{wg} v)^{3/2} \right] \qquad (8)$$

For various values of shell radii, v' from equation (8) is plotted in Figure 6, normalized to the bulk flow speed, For low shell velocity, v -0, the average comet frame velocity is simply u_{wg}. At v large compared to u_{wg}, the average velocity is approximately v and in all directions in the comet frame. Thus v' takes account of the increased ion path lengths due to the gyrating orbits, and gives a significant correction to u_{wg} in the loss term for ions at large shell velocities in the distribution.

As the first step in modelling of the observed pickup ion distributions, the appropriate level of velocity diffusion is considered. in Figure 7 a comparison of modelling with different diffusion coefficients is presented. All plots show the second distribution of the pair considered (see Figure 3) as a solid line, and the results obtained by starting with distribution 1 and running the model from position 1' to 2. The models in Figure 7 are with source and diffusion terms only (upper panels) and also for inclusion of the loss term to give the best possible fit for the given level of diffusion (lower panels). The slope of the resulting mode] distribution is determined by the diffusion coefficient, as seen in the figure. We arc particularly concerned with obtaining a good fit at shell velocities above the injection peak. It is found that the best fit diffusion coefficient is fairly low, D_0 -0.005, because larger rates modify the shape of the distribution to an extent where the slope can no longer be fitted by the loss term; this therefore constrains the model.

Example "best fit" model results are shown in Figure 8 for modelling with source, diffusion, and loss terms. In each example the data are plotted in the same format as in Figure 3, and the overlayed heavy dashed line is the modelled approximation to the solid line. Note that the accelerated ion phase-space region above the peak is of interest here, and it is not possible to fit low $v < |v_{inj}|$ accurately probably because collisional effects important in the core of the distribution [*Puhl et* al., 1993] have been ignored. However, ion losses in the core region are smaller since the loss term depends on v. The best fit at $v > |v_{inj}|$ is provided by a loss term with σ ~2 to 7 X 10^{-14} cm^2, an order of magnitude or more greater than the usual value of $\sigma \sim 2 \times 10^{-15}$ cm^2. It is therefore apparent that in addition to unexpectedly high total water group ion densities, there also appears to be considerable losses to the energetic implanted ions in this region of the cometosheath.

The ion depiction may also be expressed as $n_i v_L$ in terms of a loss rate, v_L, which is perhaps equivalently a fast neutral production rate, (This description is similar to the production rate N_c v of ions from the ionization of the outgassing neutrals.) If this were replaced for the loss term in equation (3) then during the numerical run from distribution 1 to model distribution 2 the total ion density lost is described by $n_i v_L (dx/u_{wg})$, where dx is the distance between position 1' and 2. This can be estimated directly as the number density of ions represented by the shaded area in Figure 3, or if the effect of diffusion is to be considered then the difference between the model and distribution 2 is required where the model is run without a loss term (e.g., upper left plot in Figure 7). Thus v_L may be estimated from

$$\sum_{v > v_{inj}} 4\pi v^2 \left(F_1(v) - F_2(v)\right) dv = n_i v_L \frac{dx}{u_{wg}} \qquad (9)$$

for each of the distribution pairs. Results for all of the IMS distributions in the region of interest are plotted in Figure 9 (top panel), The calculations are performed for F_2 as both the observed distribution 2 (result labelled DO= 0.0 in Figure 9) and the model with

diffusion coefficient $D_0 = 0.005$. The comparison gives some idea of the level of uncertainly in the analysis and interpretation. The loss rate for water group ions is of the order of 1 to 2 xl $0'^4$/s and appears to vary, with highest values at distances around the magnetic pileup boundary (1.35x 10^5 km), and lower at both ends of the region considered. Coincidence of maximum rates with the magnetic pileup boundary perhaps suggests the effect may partly be related to field configurations, which are not considered in the present model,

The lost flux of particles (or flux of fast neutrals created) may be calculated from $\int_{x_0}^{\infty} n_i \nu_L \, ds$ where n_i is itself obtained from the integral in equation (2) and ν_L is undoubtedly distance dependent, We can approximate this by summing the contributions to the flux found between each successive distribution pair, assuming there is little contribution from further upstream (where IMS HERS water group distributions arc not avai lable). The resul ts arc presented in the lower panel of Figure 9. For comparison, the dashed line is the flux obtained from $\sum n_i \nu_L \, dx$ for a constant ν_L of 1 x 10-4 /s, The flux production appears to fall off inside of - 1 x 10S km. It should be remembered that these estimates assume all the lost ions become neutralized (which may not be the case) and also do not take into account the subsequent losses to the fast neutral particles as they participate in further interactions. Also it is difficult to estimate an accurate bulk velocity for the particle flux, firstly because the loss rate probably varies with $|\mathbf{u}_{wg} - \mathbf{v}|$ around the shell and also, once neutralized, the particles are decoupled from the massloading deceleration of the charged plasma. However, the flux estimates should prove useful for future investigations of the effects of fast neutrals in cometosheath region processes and development of more detailed chemical models.

4. SUMMARY

In the Halley midcometosheath region (-0,5 to 2.5x 10^5 km), where ion densities reach unexpectedly high levels, the loss rate of energetic implanted ions appears to be faster than can be explained with the usual cross-sections for charge exchange interactions with the expanding cometary gas. "l'he modelling of the pickup ion distributions results in the following three empirical parameters:

(*a*) An approximation to the average ion production rate in this region is provided by an ionization rate of vi - 3 x 10-6/s in the simple 1 I) model used to calculate the i mplanted ion flux. This is significantly higher than the value of ν_i - 10^{-6}/s used in standard models. In order to compare the ion production with the depletion of cometary neutrals, the neutral mass spectrometer (NMS) water vapor data [*Krankowsky et al., 1986]* arc presented in Figure 10. The best fit to the H_2O data is provided by $Q = 5.5 \times 10^{29}$ / s and ν -2 x 10"5 /s in the simple model of equation (1). This Q_{H_2O} was obtained by *Krankowsky et al. [1986].* For H_2O the total loss rate v includes dissociation (to produce OH and O) as well as ionization. Also shown in Figure 10 is the implied total water group neutral density profile required (for depletion corresponding to ionization) to produce the observed implanted ion flux, i e., with parameters Q = 5.5x 1029/s and vi ~ 3 x 10^{-6} /s. This also implies high total dissociation rates for H_2O in terms of our simple model, however the different expansion velocities of OH and O after dissociation would modify rate estimates. Other possible mechanisms for loss of H_2O include 'clumping' of water molecules or their destruction by impacts with dust.

(*b*) The best-fit diffusion coefficient is D_0 = 0.005 kJn^2 S^{-3}, which represents a lower diffusion rate than in other models. For example, the D_{vv} coefficients used by *Gombosi et al. [1991]* just outside the Halley bow shock (his Figure 3) correspond to a D_0 - 0.007 km^2 S^{-3} in terms of our present model. This coefficient is perhaps not significantl y higher, given the uncertainty of the present modelling. However, in the

1 lalley cometosheath, the velocity diffusion modelled by *Puhl et al.* [1993] is considerably higher, equivalent to a $D_0 \sim 0.08$ at $r \sim 1$ to 1.5 x 0^5 km, as apparent from the level of broadening seen in his Figure 6*a*.

(c) The loss rate expressed as a charge exchange with outgassing cometary neutrals gives a cross-section $\sigma \sim 2$ to 7 $x 10^{-14}$ cm^2 in the present model. Losses in this region of the cometosheath therefore appear to be over an order of magnitude faster than can be explained with the standard $\sigma \sim 2 x 10^{-15}$ cm^2. Modelling in terms of flux gives an estimate of the ion loss rate ν_I of the order of 10^{-4} /s, which would equivalently be a rate for creation of fast neutral particles if charge exchange were the only significant loss mechanism. The flux of fast neutrals may contribute to the effects of: (1) increased ionization rates duc to electron knock-out collisions with the expanding neutral gas, (2) creation of the observed negative ions, and (3) the fast ions observed in the magnetic cavity. Fast neutrals may subsequently be reionized, perhaps after deceleration by multiple collisions.

Limitations of the present model include the neglect of other possible ion acceleration processes (e.g., adiabatic acceleration), the neglect of Coulomb collisions which would drive the core of the distribution toward a maxwellian [e.g., *Puhl et al., 1993],* and treatment of the water group as a whole with constant gas expansion and ionization parameters. Also wc have not included possible effects of deflected flowlines and magnetic field draping configurations which may be a significant factor close to the magnetic pileup boundary. Solar wind and pickup protons may aiso be neutralized to contribute to the fast neutral flux, but arc unlikely to have much of an effect on cometosheat h processes since their momentum is much less t ban that of heavy cometary ions. Another consideration is the significant flux of keV electrons [*Larson and Lin*, 1992; D. E. I arson, private communication 1993] observed upstream of cometocentric distance r - 10^5 km, which can cause electron impact ionization and hence contribute to the observed high flux of implanted ions along the flowlines. The present model has

provided estimates for rates of ionization and ion velocity diffusion processes in the Halley midcometosheath, and estimates of the fast neutral flux. For the future, further development of multispecies chemical models in combination with detailed fluid descriptions may help to explain the ion density observations near the magnetic pileup boundary.

Acknowledgments We thank D. Krankowsky and R.R. Hodges, Jr., for use of the NMS data in Figure 10. This paper represents one aspect of research carried out at the Jet Propulsion Laboratory of the California Institute of Technology under contract to the National Aeronautics and Space Administration. DEH was supported by the Resident Research Associate Program of the National Research Council.

REFERENCES

Altwegg, K., H. Balsiger, J. Geiss, R. Goldstein, W.-H. lp, A. Meier, M. Neugebauer, H. Rosenbauer, and E. Shelley, The ion population between 1300 km and 230,000 km in the coma of comet P/Halley, *Astron. and Astrophys., in press, 1993.*

Coates, A. J., B. Wilken, A. D. Johnstone, K. Jockers, K.-H. Glassmeier, and D. E. Huddleston, Bulk properties and velocity distributions of water group ions at cornet Halley: Giotto measurements, *J. Geophys. Res.,* 9.5, 10249, 1990.

Eberhardt, P., D. Krankowsky, W. Schulte, U. 1 Dolder, P. Lämmerzahl, J. J. Berthelier, J. Woweries, U. Stubbemann, R. R. Hodges, J, H. Hoffman, and J. M. Illiano, The CO and N_2 abundance in comet P/Halley, *Astron. Astrophys., 187, 481,* 1987.

Eviatar, A., R. Goldstein, D. T. Young, H. Balsiger, H. Rosenbauer, and S. A. Fuselier, Energetic ion fluxes in the inner coma of comet P/Halley, *Astrophys. J.,* 339, 545, 1989.

Galeev, A. A., Theory and observations of solar wind/cometary plasma interaction processes, in: *Proc. of 20th ESLAB Symposium on the Exploration of Halley's Comet,* edited by B. Battrick, E. J, Rolfe and R. Reinhard, *Vol. I,* pp. 3, ESA S1'-250, Heidelberg, Germany, 1986.

Galeev, A. A., and R. Z. Sagdeev, Alfvén waves in a space plasma and its role in the solar wind integration with comets, *Astrophys. Space Sci., 144, 427,* 1988,

Glassmeier, K.-}]., A. J. Coates, M. }1. Acuña, M, L. Goldstein, A. D. Johnstone, F. M. Neubauer, and H. Reme, Spectral characteristics of low-frequency plasma turbulence upstream of comet P/1 Ialley, *J. Geophys. Res.,* 94, 37, 1989.

Gombosi, T. 1., Preshock region acceleration of implanted cometary H^+ and O^+, *J. Geophys. Res.,* 93, 35, 1988.

Gombosi, T. *1.*, M. Neugebauer, A. D. Johnstone, A. J. Coates, and D. E. Huddleston, Comparison of Observed and Calculated Implanted Ion Distributions Outside Comet Halley's Bow Shock, *J. Geophys. Res., 96*, 9467, 1991.

Hodges, R. R., Jr., Monte Carlo simulation of nonadiabatic expansion in cometary atmospheres: Halley, *Icarus, 83, 410,* 1990.

Huddleston, D. E., A. D. Johnstone, and A. J. Coates, Determination of comet Halley gas emission characteristics from mass loading of the solar wind, *J. Geophys. Res.,* 95, 21, 1990.

Huddleston, D. E., A. J. Coates, and A. D. Johnstone, Quasi-1 inear velocity space diffusion of heavy cometary pickup ions on bispherical diffusion characteristics, *J. Geophys. Res., 97, 19,163, 1992.*

Huddleston, D. E., and A. D. Johnstone, Relationship between wave energy and free energy from pickup ions in the comet Halley environ ment, *J. Geophys. Res.,* 97, 12,217, 1992.

Huddleston, D. E., M. Neugebauer, and B. E. Goldstein, Water group ion distributions in the midcometosheath of cornet Halley, *J. Geophys. Res., 98, 21,039, 1993.*

Isenberg, P. A., Energy diffusion of pickup ions upstream of cornets, *J. Geophys. Res.,* 92,8795, 1987.

Krankowsky, D., P. Lämmerzahl, I. Herrwerth, J. Woweries, P. Eberhardt, U. Dolder, U. Herrmann, W. Schulte, J. J. Berthelier, J. M. Illiano, R. R. Hodges, and J. H. Hoffman, *In situ* gas and ion measurements at comet Halley, *Nature,* .?21, 326, 1986.

Larson, D. E., and R. P. 1 in, Observations of low energy electrons inside the cometosheath of cornet Halley (abstract), *EOS Trans. AGU, 7.?,* Fall Meeting suppl., 438, 1992.

Meier, R., P. Eberhardt, D. Krankowsky, and R. R. Hodges, The extended formaldehyde source in cornet P/1 Ialley, *Astron. Astrophys., in press, 1993.*

Miller, R.H., S. P. Gary, D.Winske, and T. I. Gombosi, l)itch-angle scattering of cometary ions into monospherical and bispherical distributions, *Geophys. Res. Lett., 18*, 1063, *1991.*

Mukai, T., W. Miyake, l'. Terasawa, M. Kitayama, K, Hirao, Plasma observation by Suisei of solar wind interaction with comet Halley, *Nature, 321*, 299, 1986.

Neugebauer, M., R. Goldstein, B. E. Goldstein, S. A. Fuselier, H. Balsiger, and W.-H. Ip, Densities and abundances of hot cometary ions in the coma of P/Halley, *Astrophys. J.*, .?72,291, 1991.

Pubj, P., T. E. Cravens, and J. Lindgren, Ion thermalization in the inner coma of a cornet, *Astrophys. J., 418, 899,* 1993.

Sagdeev, R. Z., V. D. Shapiro, V. 1. Shevchenko, and K. Szegö, MHD turbulence in the solar wind - cornet interaction region, *Geophys. Res. Lett., 13*, 85, 1986.

Schmidt, H. U., R. Wegmann, W. F. Huebner, and D. C. Boice, Cometary gas and plasma flow with detailed chemistry, *Comp. Phys. Comm.*, 49, 17, 1988.

Wu, C. S., and R. C. Davidson, Electromagnetic instabilities produced by neutral particle ionization in interplanetary space, *J. Geophys. Res.*, 77, 5399, 1972.

Ye, G., T. E. Cravens, and T. 1. Gombosi, Pickup protons and water ions at comet Halley: comparisons with Giotto observations, *J. Geophys. Res., 98,* 1311,1993.

FIGURE CAPTIONS

Fig. 1. Velocity-space sketch of the cometary ion bispherical shell injection distribution in the plasma frame, where $v_{||}$ anti $v_{\perp}$ arc the ion field-aligned and perpendicular velocities, respectively. θ_u and θ_d are the ring injection angles in the -VA and + V_A wave frames, respectively, α is the angle between the field and flow vectors, and V_u and V_d are the radii of the partial shell sections. (Taken from *Huddleston et al. [1993].)*

Fig. *2.* The cometary water group ion densities observed by the Giotto ion mass spectrometer in the Halley midcometosheath region. The overlayed line is the simple model fit (equation (2)) from which the ioni zat ion rate is cst i mated.

Fig. 3. Cometosheath water group ion spectra observed by the IMS HERS. The distributions arc plotted in pairs to show their development on approach to the comet, Shaded areas in each plot represent the loss of ions at $v > |v_{inj}|$.

Fig. *4.* Schematic diagram illustrating the effects of (a) pickup, (b) energy diffusion, and (c) charge exchange to be modelled in the evolution of the cometary ion spectra.

Fig. *5.* The Giotto encounter geometry at comet Halley. The dashed line represents an example model flowline on which distribution 1 is given a projected position 1‘ (see text) and used as the starting point from which distribution 2 is modelled.

Fig. 6. The effect of the plasma magnetization is shown here in terms of the relationship between the average ion shell velocity v’ in the neutral gas (comet) frame and the shell velocity radius v.

Fig. 7. Fitting the diffusion coefficient to give the best-fit slope of the $F(v)$ spectra at shell velocities above the injection peak. Results for three different coefficients arc shown here for modelling both with and without the loss term.

Fig. 8. The best-fit model results for the ion distribution pairs of Figure 3. The heavy dashed line is the model fit to the solid line. Diffusion coefficients and charge exchange rates used in each case arc given on the plots.

Fig. 9. Ion loss rates and fast neutral fluxes both for the mode] with velocity diffusion coefficient Do = 0.005 $km^2 s^{-3}$, and also for no added diffusion (denoted $D_0 = 0.0$) calculated from the shaded areas as seen in the Figure 3 examples.

Fig. 10. Comparison of the NMS water vapour neutrals [*Krankowsky et* al., 1986] with the simple model best-fit (equation (1)) and also comparison with the implied total water group neutral density profile for the same ionization rate as required to fit the ions in Figure 2.

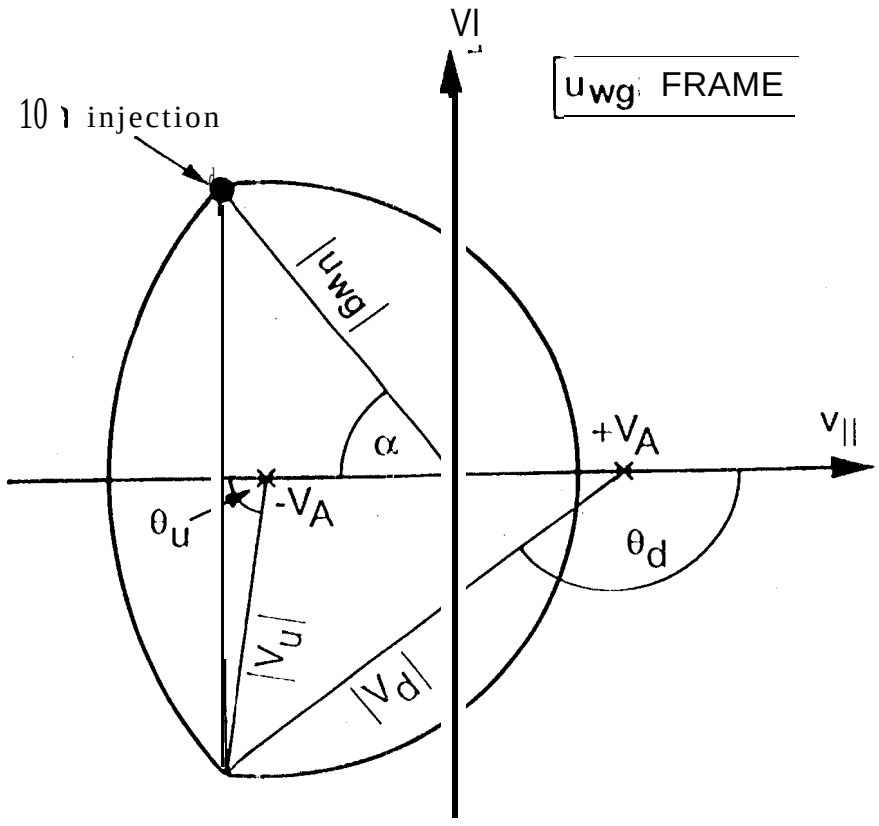

Fig. 1.

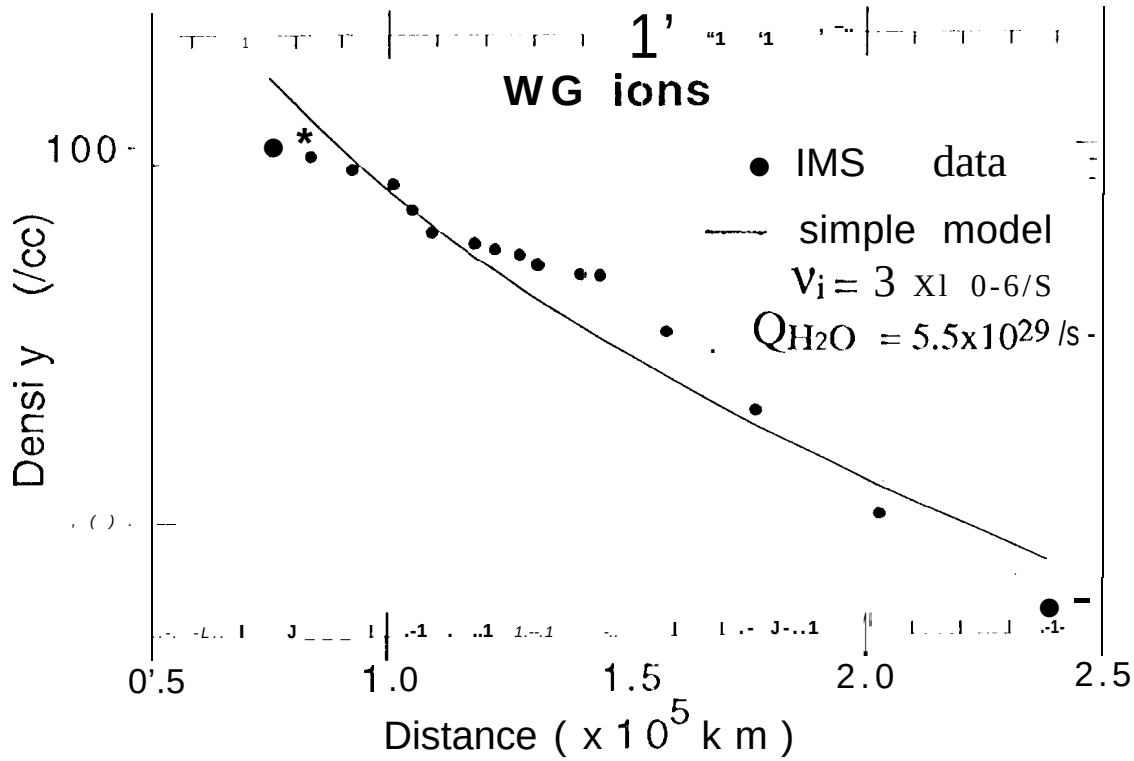
WG ions
IMS data
simple model
$\nu_i = 3$ X1 0-6/S
$Q_{H_2O} = 5.5x10^{29}$ /s
100
Densi y (/cc)
0'.5
1.0
1.5
2.0
2.5
Distance (x 1 0^5 k m)

Fig. 2.

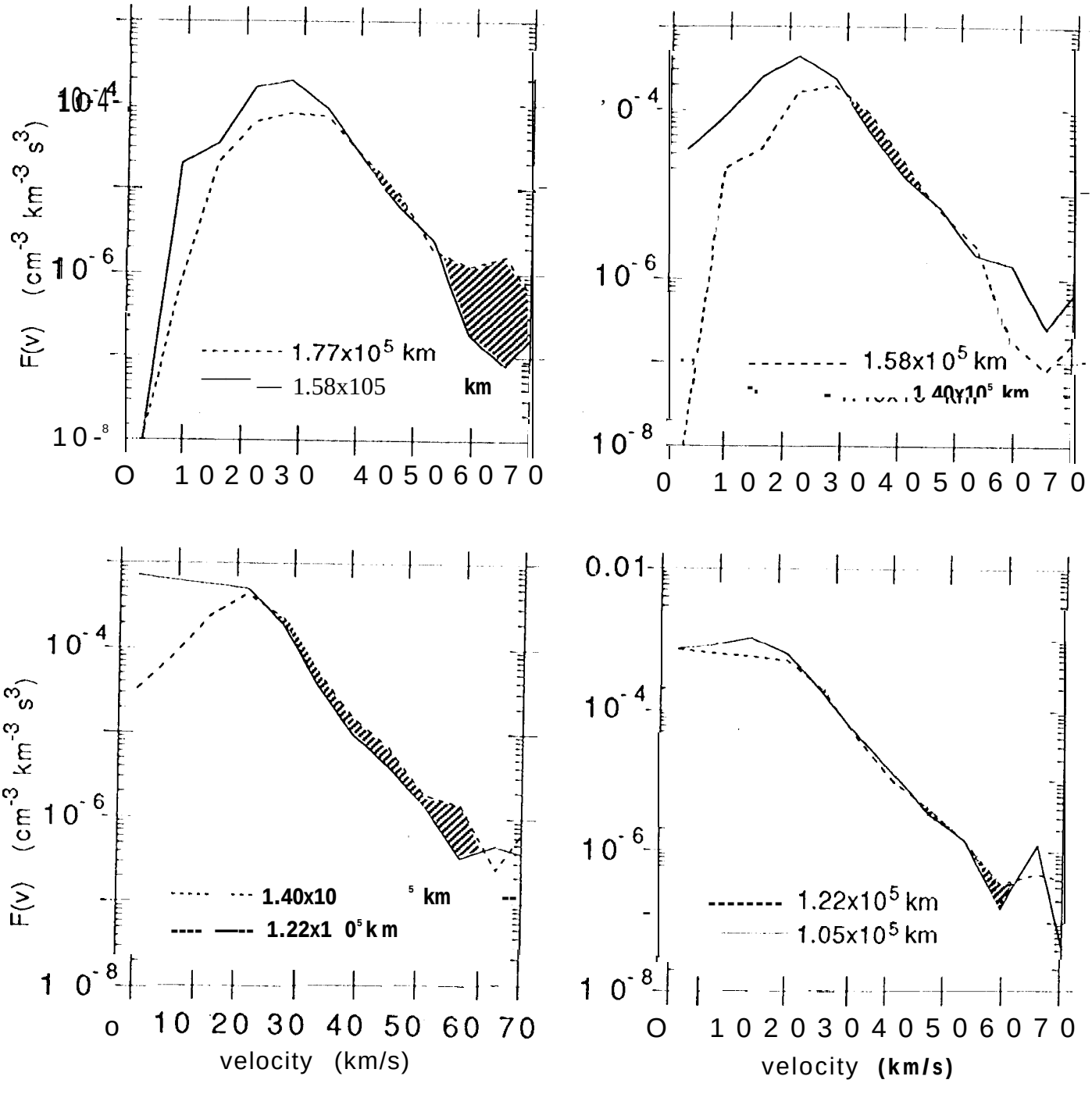
F(v) (cm-3 km-3 s3)
10-4
10-6
10-8
1.77x10^5 km
1.58x105 km
0 10 20 30 40 50 60 70
1.58x10^5 km
1.40x10^5 km
1.40x10^5 km
1.22x10^5 km
velocity (km/s)
0.01
1.22x10^5 km
1.05x10^5 km
velocity (km/s)

Fig. 3.

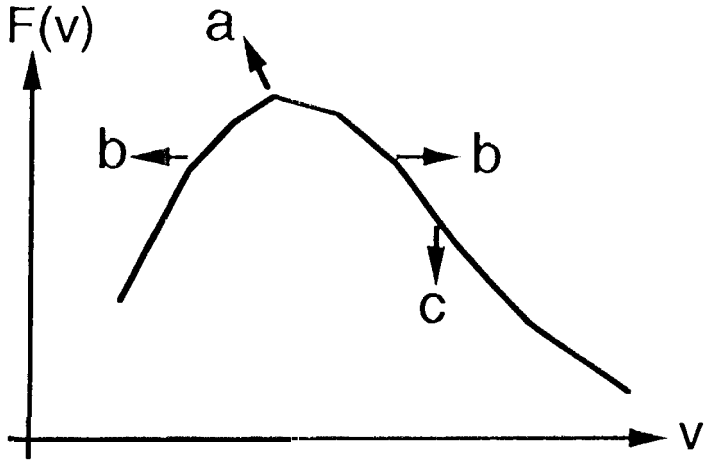

Fig. 4.

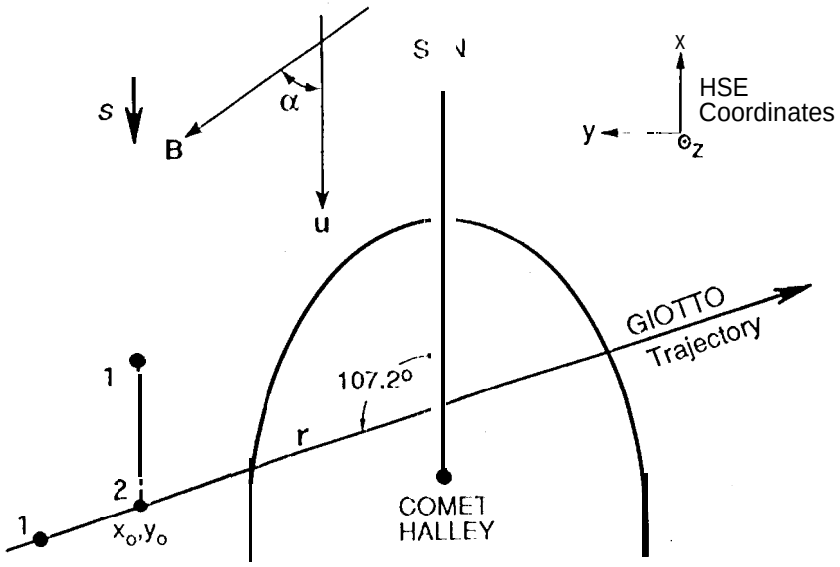
S
α
B
u
x
HSE
Coordinates
y
z
GIOTTO
Trajectory
107.2°
r
1
2
1
x_o, y_o
COMET
HALLEY

Fig. **5.**

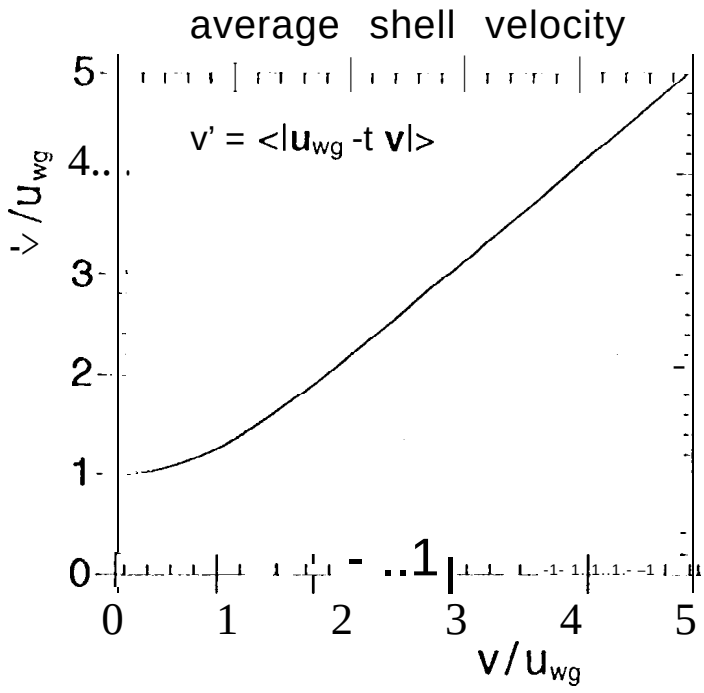

Fig. 6.

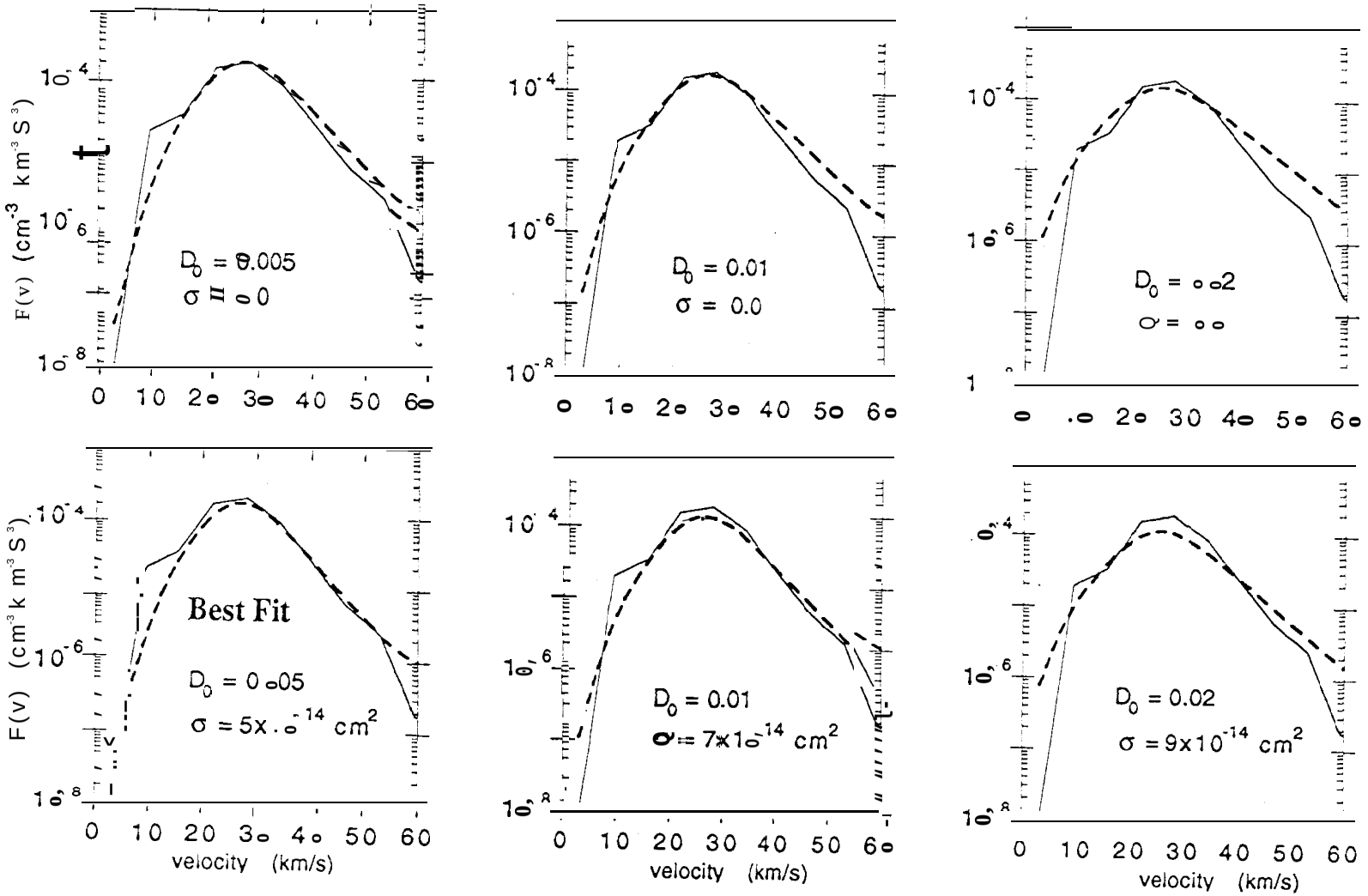
F(v) (cm-3 km-3 S3)
D0 = 0.005
σ = 0
D0 = 0.01
σ = 0.0
D0 = 0.02
σ = 0
Best Fit
D0 = 0.05
σ = 5x10-14 cm2
D0 = 0.01
σ = 7x10-14 cm2
D0 = 0.02
σ = 9x10-14 cm2
velocity (km/s)
velocity (km/s)
velocity (km/s)

Fig. 7.

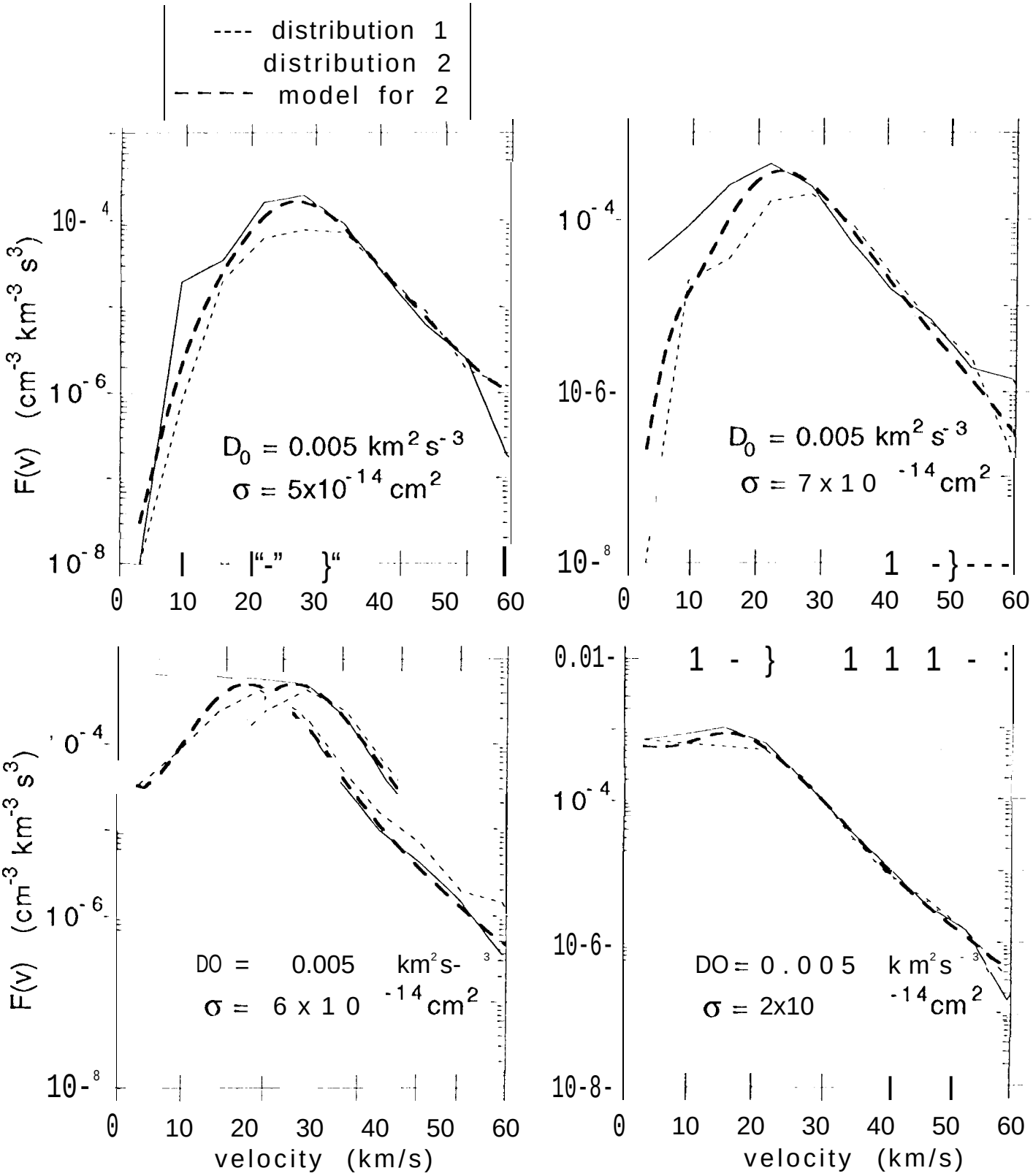
---- distribution 1
distribution 2
model for 2
F(v) (cm-3 km-3 s3)
D0 = 0.005 km2 s-3
σ = 5x10-14 cm2
D0 = 0.005 km2 s-3
σ = 7 x 10-14 cm2
DO = 0.005 km2s-3
σ = 6 x 10-14 cm2
DO = 0.005 km2s-3
σ = 2x10-14 cm2
velocity (km/s)
velocity (km/s)

Fig. 8.

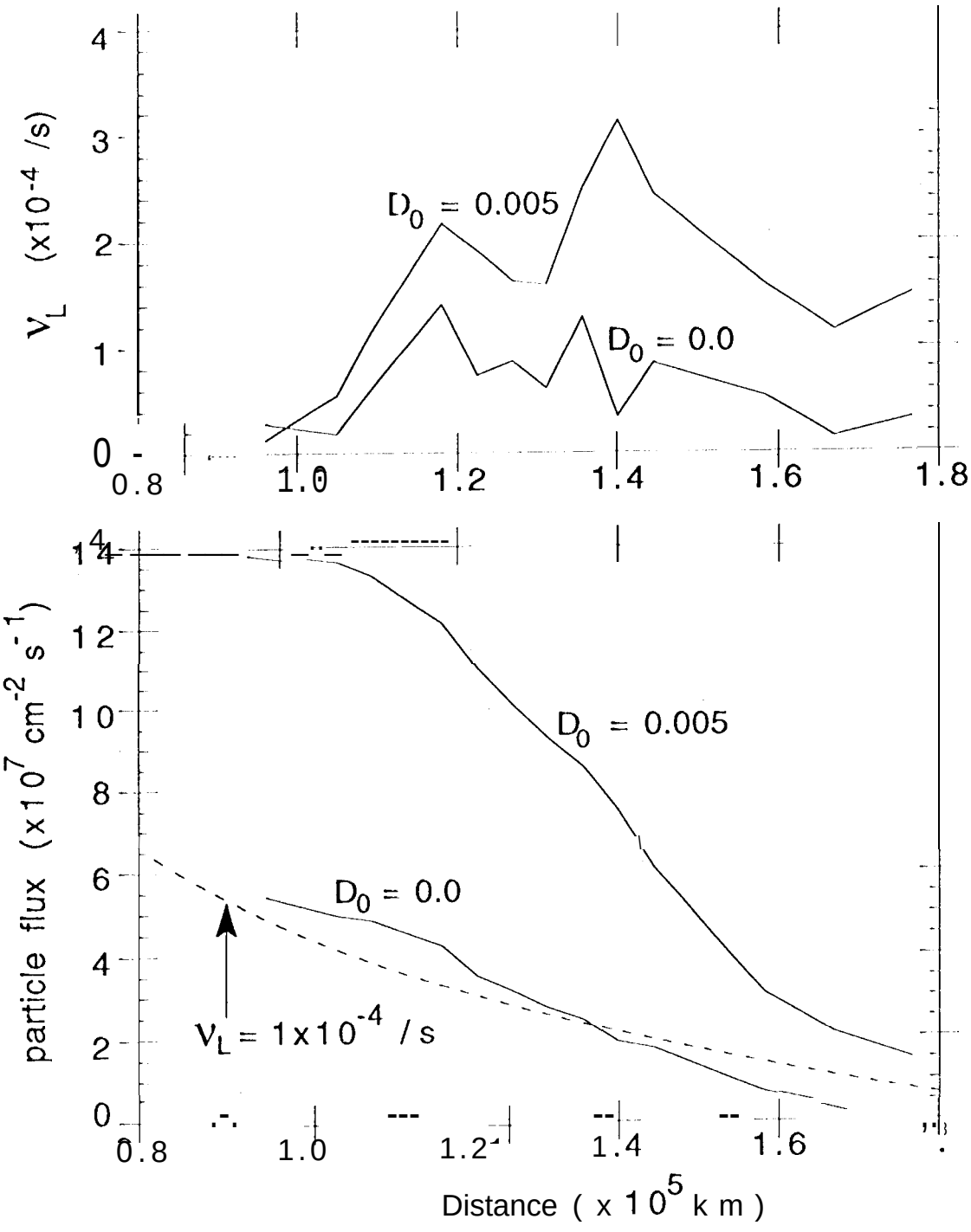
ν_L (x10^{-4} /s)
D_0 = 0.005
D_0 = 0.0
particle flux (x10^7 cm^{-2} s^{-1})
D_0 = 0.005
D_0 = 0.0
ν_L = 1x10^{-4} / s
Distance (x 10^5 k m)

Fig. 9.

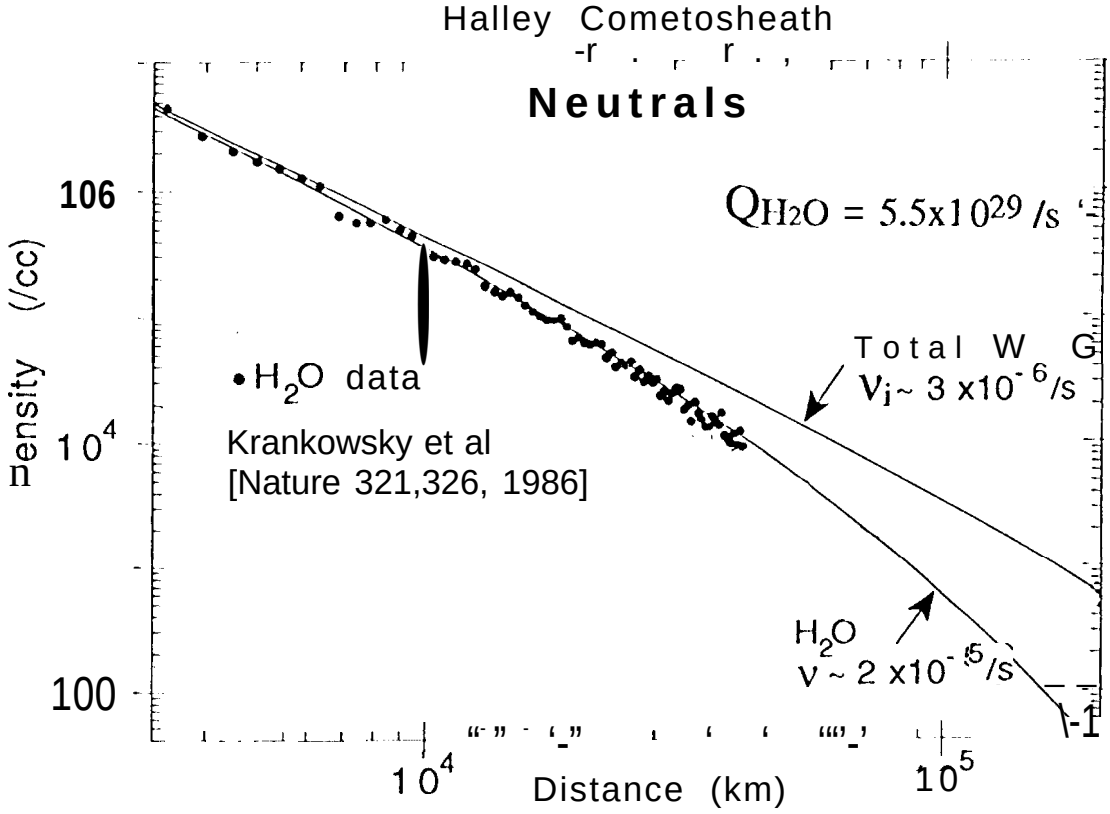
Halley Cometosheath
Neutrals
106
$Q_{H_2O} = 5.5 \times 10^{29}$ /s
Total W G
$\nu_i \sim 3 \times 10^{-6}$/s
• H_2O data
Krankowsky et al
[Nature 321,326, 1986]
H_2O
$\nu \sim 2 \times 10^{-5}$/s
100
10^4
Distance (km)
10^5
Density (/cc)

Fig. 10.